LETTER

doi:10.1038/nature11392

Activation of old carbon by erosion of coastal and subsea permafrost in Arctic Siberia

J. E. Vonk[1]†*, L. Sánchez-García[1]†*, B. E. van Dongen[1]†, V. Alling[1]†, D. Kosmach[2], A. Charkin[2], I. P. Semiletov[2,3], O. V. Dudarev[2], N. Shakhova[2,3], P. Roos[4], T. I. Eglinton[5], A. Andersson[1] & Ö. Gustafsson[1]

The future trajectory of greenhouse gas concentrations depends on interactions between climate and the biogeosphere[1,2]. Thawing of Arctic permafrost could release significant amounts of carbon into the atmosphere in this century[3]. Ancient Ice Complex deposits outcropping along the ~7,000-kilometre-long coastline of the East Siberian Arctic Shelf (ESAS)[4,5], and associated shallow subsea permafrost[6,7], are two large pools of permafrost carbon[8], yet their vulnerabilities towards thawing and decomposition are largely unknown[9–11]. Recent Arctic warming is stronger than has been predicted by several degrees, and is particularly pronounced over the coastal ESAS region[12,13]. There is thus a pressing need to improve our understanding of the links between permafrost carbon and climate in this relatively inaccessible region. Here we show that extensive release of carbon from these Ice Complex deposits dominates (57 ± 2 per cent) the sedimentary carbon budget of the ESAS, the world's largest continental shelf, overwhelming the marine and topsoil terrestrial components. Inverse modelling of the dual-carbon isotope composition of organic carbon accumulating in ESAS surface sediments, using Monte Carlo simulations to account for uncertainties, suggests that 44 ± 10 teragrams of old carbon is activated annually from Ice Complex permafrost, an order of magnitude more than has been suggested by previous studies[14]. We estimate that about two-thirds (66 ± 16 per cent) of this old carbon escapes to the atmosphere as carbon dioxide, with the remainder being re-buried in shelf sediments. Thermal collapse and erosion of these carbon-rich Pleistocene coastline and seafloor deposits may accelerate with Arctic amplification of climate warming[2,13].

The large magnitude of shallow permafrost carbon pools relative to the atmospheric pools of carbon dioxide (~760 Pg) and methane (~3.5 Pg) suggests that carbon release from thawing permafrost has the potential to affect large-scale carbon cycling. Arctic permafrost can be divided into three main compartments: terrestrial (tundra and taiga) permafrost (~1,000 Pg C)[8], Ice Complex (coastal and inland) permafrost (~400 Pg C)[4,8] and subsea permafrost (~1,400 Pg C)[6,7]. Even without considering subsea permafrost, the carbon held in the top few metres of the pan-arctic permafrost constitutes approximately half of the global soil organic carbon pool[8].

Investigations of Arctic greenhouse gas releases have focused on terrestrial permafrost systems[4,9,15], and only recently on subsea permafrost[6,7,16,17], with a notable scarcity of studies on the thawing permafrost outcropping along the Arctic coast. In particular, the extensive coastline of the Eastern Siberian Sea (ESS) is dominated by exposed tall bluffs comprising ice-rich, fine-grained Ice Complex deposits (Fig. 1a). The origin of the ~1-million-km^2 deposits (with average depth 25 m) dominating northeastern Siberia (and parts of Alaska and northwestern Canada) is under some debate, but this Pleistocene material is quite distinct from peat and mineral soil of other Arctic permafrost[4,5]. These relict soils of the steppe-tundra ecosystem have high carbon contents (1–5%)[4,5]. The export of organic carbon from the eroding ESAS Ice Complex is presently estimated at 4 Tg yr^{-1} (ref. 14), yet it has also been proposed that erosion from the Lena Delta coastline alone might contribute this amount[18]. Clearly, large uncertainties remain regarding the magnitude of eroded carbon export from land to the shelf.

The extensive coastal exposure of the Ice Complex deposits (ICD) makes them potentially more vulnerable than other terrestrial permafrost; ICD retreat rates are 5–7 times higher than those of other coastal permafrost bodies[18]. A destructive thaw-erosion process brought on by thermal collapse of the coastline promotes surface

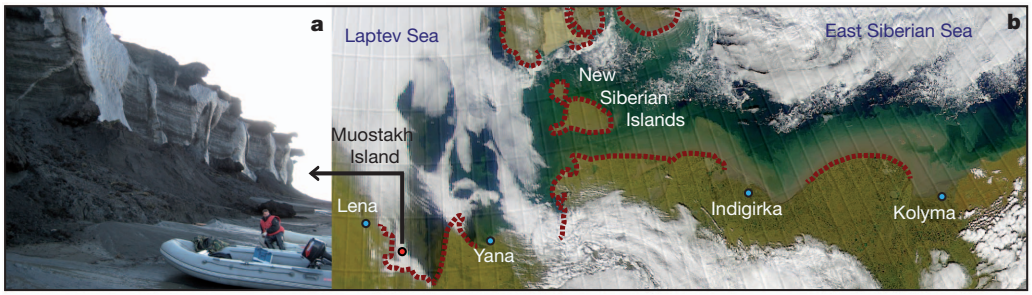

Figure 1 | Erosion of Ice Complex deposits on the East Siberian Arctic Shelf. **a**, Eroding, carbon-rich Ice Complex coast on Muostakh Island in the southeastern Laptev Sea. **b**, Erosion-induced turbidity clouds envelop several thousand kilometres of East Siberian Sea coastal waters. Note the rounded shorelines of northeastern Siberia, indicative of coastal erosion. Red dashed line shows areas of intensive ongoing erosion. (Satellite image of 24 August 2000, available at http://visibleearth.nasa.gov.)

[1]Department of Applied Environmental Science (ITM) and the Bert Bolin Centre for Climate Research, Stockholm University, Svante Arrhenius väg 8, SE-11418, Stockholm, Sweden. [2]Pacific Oceanological Institute, Russian Academy of Sciences, ul. Baltiiskaya 43, 690041, Vladivostok, Russia. [3]International Arctic Research Center, University of Alaska, PO Box 757335, Fairbanks, Alaska 99775-7335, USA. [4]Risø National Laboratory for Sustainable Energy, Frederiksborgvej 399, 4000, Roskilde, Denmark. [5]Geological Institute, ETH-Zürich, Sonneggstrasse 5, CH-8092, Zürich, Switzerland. †Present addresses: Geological Institute, ETH-Zürich, Sonneggstrasse 5, CH-8092, Zürich, Switzerland (J.E.V.); Catalan Institute of Climate Sciences (IC3), C/Doctor Trueta 203, 08005, Barcelona, Spain (L.S.-G.); School of Earth, Atmospheric and Environmental Sciences, The University of Manchester, Oxford Road, Manchester M13 9PL, UK (B.E.v.D.); Norwegian Geotechnical Institute, Sognsveien 72, 0855, Oslo, Norway (V.A.).
*These authors contributed equally to this work.

subsidence, with ICD loss exacerbated by the increased wave and wind erosion that accompany sea-level rise and longer ice-free seasons[2]. Satellite images show a large erosional turbidity cloud along the ESAS coastline (Fig. 1b). From limited land-based surveys, this ICD erosion is thought to be delivering as much total organic carbon to the ESAS as all its large rivers combined[19,20]. Unfortunately, these studies are limited in spatial coverage, and do not consider the fate of the released carbon in the receiving ocean. There are no field-based reports of degradation or greenhouse-gas releases of thawing ICD; however, a recent investigation of organic matter genesis in ESS surface sediments suggests that ICD erosion may dominate over planktonic and riverine sources[21]. Laboratory experiments have shown that microbial degradation begins once permafrost has thawed, implying survival of viable bacteria and an inherent lability of the very old ICD organic carbon (ICD-OC)[10,11]. In addition to terrestrial ICD, the ESAS sediments (inundated by seawater during the early Holocene epoch) also host large Pleistocene deposits, presumably containing carbon in quantities similar to those in the upper-1-m soil pool[6,8]. These reservoirs are subject to active sea-floor thermal erosion[16,17], potentially releasing as much organic carbon as coastal erosion and rivers[20]. Overall, carbon released from thawing and eroding coastal permafrost may play a quantitatively important role in the Arctic carbon cycle.

To evaluate the role of the ICD and subsea permafrost carbon (hereafter jointly referred to as ICD-PF) in the contemporary ESAS carbon cycle, we adopted an inverse approach based on deducing the contribution of this ICD-PF to carbon accumulating on the entire ESAS shelf. We analysed more than 200 sediment samples (see Methods Summary), collected during ship-based expeditions spanning the ESAS (Supplementary Fig. 2, Supplementary Methods). We used a dual-carbon-isotope ($\delta^{13}C$ and $\Delta^{14}C$) mixing model, solved with a Monte Carlo simulation strategy to account for endmember uncertainties, to deconvolve the relative contributions from ICD-PF, plankton detritus and a terrestrial/topsoil component. We then combined the fractional contribution from ICD-PF with the radiochronologically constrained sediment accumulation flux (Methods Summary and Supplementary Methods) to derive the shelf-wide re-burial flux of old carbon from permafrost.

We examined the fate of thawing ICD-OC in ambient conditions on coastal slopes of Muostakh, an island in the southeastern Laptev Sea that is disappearing as a result of erosion rates of up to 20 m yr^{-1} (refs 19,20,22; Fig. 1a). Bulk carbon contents, and molecular and isotopic compositions of ICD-OC, were assessed in conjunction with *in situ* CO_2 evasion fluxes (Supplementary Methods) to assess susceptibility of the organic carbon to degradation before delivery into coastal waters.

Radiocarbon ages of surface-sediment organic carbon ranged between 10,800 and 7,300 ^{14}C yr (Fig. 2a shows $\Delta^{14}C$ values; see also Supplementary Table 1) in the western ESS and the Dmitry Laptev Strait, regions dominated by coastal erosion (Fig. 1b). Organic-carbon radiocarbon ages were also old in the southern ESS and the Laptev Sea, ranging from 7,800 to 3,200 ^{14}C yr. Lateral shelf transport times are likely to be much smaller than these measured ^{14}C ages[23], implying significant supply of pre-aged carbon to these sediments. $\delta^{13}C$ values varied, from −28.3 to −25.2‰ near the coast, to −24.8 to −21.2‰ on the outer ESAS (Fig. 2b; Supplementary Table 1). In contrast to other world-ocean shelf seas, where the sediment organic carbon originates from planktonic and riverine sources, coastline and sediment erosion represent significant sources of organic carbon to the ESAS. The relative contribution of the three sources was deduced from their carbon isotope fingerprints. In addition to a marine source, with $\delta^{13}C = -24 \pm 3.0$‰ and $\Delta^{14}C = 60 \pm 60$‰ (mean ± standard deviation (s.d.); Supplementary Methods, Supplementary Figs 4, 5), we distinguish between two terrestrial sources: ICD-PF organic carbon (coastal, inland, and subsea; formed before inundation), with $\delta^{13}C = -26.3 \pm 0.67$‰ and $\Delta^{14}C = -940 \pm 84$‰ (Supplementary Fig. 4, Supplementary Table 4), and topsoil permafrost (topsoil-PF)

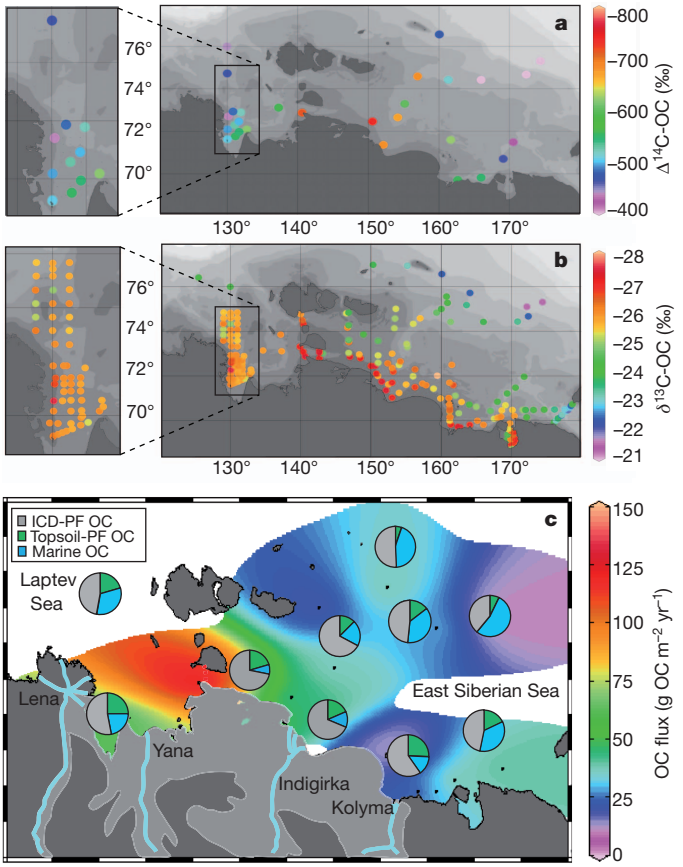

Figure 2 | Carbon isotope compositions and contribution of organic carbon sources to sediment accumulation on the East Siberian Arctic Shelf. **a**, **b**, $\Delta^{14}C$-OC (**a**) and $\delta^{13}C$-OC (**b**) signals in ESAS surface sediments. **c**, Annual sedimentary organic carbon accumulation fluxes (g OC m^{-2} yr^{-1}) and relative contributions (pie charts) of the three source pools to the surface-sediment organic carbon on the ESAS. The mean ESS contributions are: 57 ± 1.6% from ICD-PF (grey), 16 ± 3.4% from topsoil-PF (green) and 26 ± 8.0% from marine/planktonic organic carbon (blue), as identified by numerical (Monte Carlo) simulations of the dual-carbon-isotope ($\delta^{13}C$ and $\Delta^{14}C$) and endmember mixing models. Land area marked in light grey indicates the distribution of the Ice Complex[30].

organic carbon (drained from vegetation debris and the thin, surficial, annual thaw layer of the continuous permafrost regions of northeast Siberia), with $\delta^{13}C = -28.2 \pm 1.96$‰ and $\Delta^{14}C = -126 \pm 54$‰ (Supplementary Fig. 4, Supplementary Table 3 and Supplementary Methods). The endmember source assignments are based on an extensive compilation of circum-arctic literature data, yielding statistically robust and distinctive values for the three endmembers, as further explained in the Supplementary Information (Supplementary Text; Supplementary Figs 4, 5; Supplementary Tables 3, 4). Naturally, the isotopic endmember values carry uncertainties, which may be reduced in the future by additional observations of the marine and topsoil composition. The ^{13}C and ^{14}C compositions of the three endmembers are well separated from each other (Supplementary Fig. 4), which allows separation of their contributions while properly accounting for the associated uncertainties using the Monte Carlo simulation approach. We stress that the two terrestrial endmembers are solely source-based, and independent of transport or mobilization route, meaning that both ICD-PF and topsoil-PF can be delivered by coastal, delta and riverbank erosion as well as river transport. The resulting isotopic mass-balance model shows contributions of marine (planktonic) organic carbon to the shelf sediments ranging between 7% nearshore and 54% on the outer shelf, whereas topsoil-PF contributes ~30–35% close to land, decreasing to ~5% farther out (Fig. 2c).

ICD-PF constitutes 36–76% of the sedimentary organic carbon throughout the broad shelf, despite its largely coastal delivery. ICD-OC is ballasted by mineral association and rapidly settles[21,24], whereupon it is probably resuspended from the sea floor and dispersed over the shelf, mostly by bottom-boundary-layer transport[21,25,26]. Old permafrost-released erosional carbon thus dominates burial of organic carbon on the ESAS.

We estimate the net sediment burial of ICD-PF carbon using accumulation fluxes from sediment cores (36 ± 17 g OC m^{-2} yr^{-1}; all confidence intervals are 95%, unless otherwise stated; Fig. 2c, Supplementary Table 2). This was scaled up by the fraction of sea floor that is available for carbon burial (0.6), corresponding to water depth >30 m (Supplementary Fig. 2), where resuspension is negligible and sediments thus accumulate[26]. Combining the ESS shelf area (9.87×10^5 km^2) with the ICD-PF contribution to the sediment organic carbon (ESS only: 57 ± 1.6%; Supplementary Table 5) yields an overall annual ICD-PF carbon accumulation flux of 12 ± 8 Tg C yr^{-1}. Inclusion of the Laptev Sea increases this value to 20 ± 8 Tg C yr^{-1} (Supplementary Table 6). Hence, this approach reveals that the supply of carbon from ICD-PF erosion to the ESAS is much larger than has previously been assumed[14,19,20].

The biogeochemical composition of the eroding slopes of Muostakh Island (Fig. 3) indicates extensive organic matter degradation of the thawing ICD before delivery to the ocean. Recurring trends were observed in several properties between higher and lower elevations on the investigated slopes that are consistent with continuing degradation (Fig. 3; Supplementary Tables 7, 8), specifically: decreasing soil organic carbon content; increasing $\delta^{13}C$ of organic carbon ($\delta^{13}C_{OC}$); decreasing $\Delta^{14}C_{OC}$; decreasing ratio of high-molecular-weight *n*-alkanoic acids to high-molecular-weight *n*-alkanes; increasing ratio of even, low-molecular-weight to odd, high-molecular-weight *n*-alkanes; and increase in atmospheric CO_2 venting, deduced from field-chamber soil respiration measurements (Supplementary Methods). These trends and fluxes contrast with prior assumptions that all thawed and erosion-mobilized ICD-OC is directly flushed into the sea without sub-aerial degradation[14,19,20]. The elemental, isotopic and molecular data imply 66 ± 16% (mean ± s.d.; Supplementary Methods) downslope degradative loss of ICD-OC.

Combining the 20 ± 8 Tg C yr^{-1} sediment re-burial flux of thawed old organic carbon with a recent estimate of water-column degradation of terrestrially derived particulate organic carbon on the ESAS of 1.4 yr^{-1} (2.5 ± 1.6 Tg C yr^{-1}; mean ± s.d.)[27] suggests an ICD-PF organic carbon flux to the marine system of 22 ± 8 Tg C yr^{-1} (Supplementary Fig. 1). Assuming an equal contribution of this flux from coastline and subsea erosion (Supplementary Table 6, which also includes 25/75% and 75/25% models), the 66 ± 16% carbon loss along the eroding coastal slopes corresponds to a carbon venting (presumably mostly CO_2) from the ICD of 22 ± 8 Tg yr^{-1} (Supplementary Fig. 1). The total remobilization of old organic carbon from thawing of ICD-PF is thus $\sim 44 \pm 10$ Tg C yr^{-1} (Supplementary Table 6; Supplementary Fig. 1).

The present assessment suggests a substantially larger flux of carbon from thawing ICD permafrost (44 ± 10 Tg C yr^{-1}; Supplementary Table 6) than has been inferred previously from exclusively land-based surveys (~ 4 Tg C yr^{-1}; no error reported)[14]. Previous estimates of ICD erosion may have been too low for several reasons, including gross upscaling from limited point measurements of ICD retreat rates[19,20,22]. In addition, upscaling using digital shoreline length data leads to considerable underestimations[28]; and potentially large inputs from retrogressive thaw slumps and slope failure[28] are excluded when elevation change data are not included in coastline retreat measurements. Finally, bottom erosion is a previously neglected but potentially important contributor of old eroded organic carbon to the modern biogeochemical cycle on the ESAS, with erosion rates of 10–30 cm yr^{-1} (refs 18,29) at depths less than 30 m (nearly half the ESAS), where present-day bottom-water temperatures in summer are 2–3 °C and

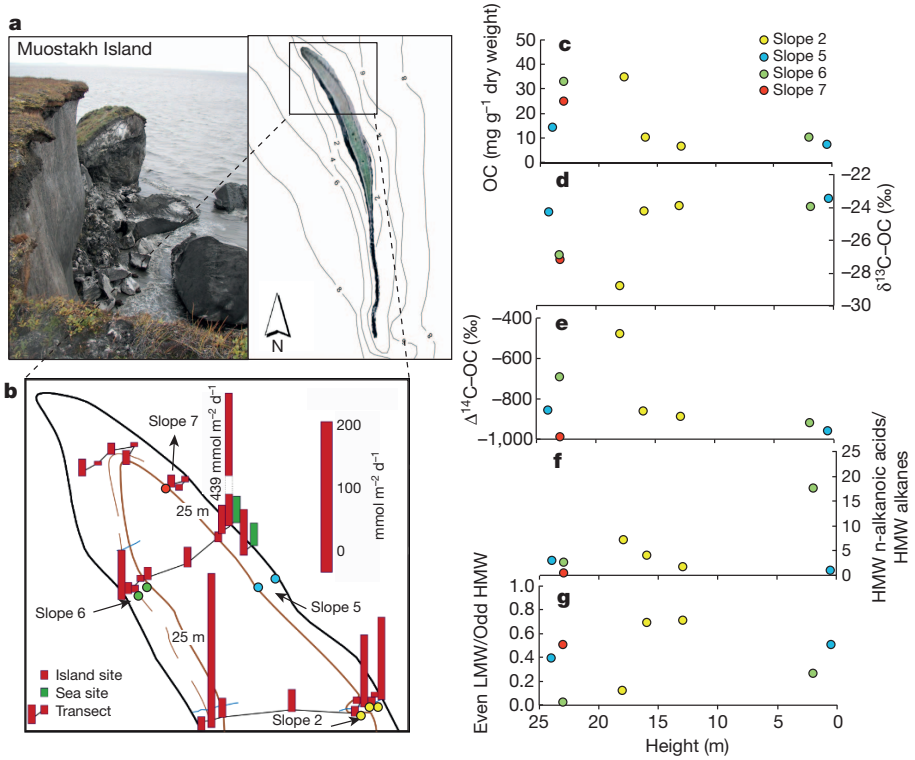

Figure 3 | Biogeochemical signals of Ice Complex organic matter degradation on Muostakh Island. **a**, Study area. **b**, Distribution of CO_2 outgassing. **c–g**, Distributions along the four studied slopes (positions indicated in **b**) of soil organic carbon content (**c**); δ^{13}C-OC signal (**d**); Δ^{14}C-OC signal (**e**); ratio of high-molecular-weight *n*-alkanoic acids to high-molecular-weight *n*-alkanes (proxy for degradation status) (**f**) and ratio of even, low-molecular-weight *n*-alkanes to odd, high-molecular-weight *n*-alkanes (proxy for bacterial biomass relative to substrate) (**g**). Ratios in **f** and **g** are molecular ratios.

have risen during the past decade[13]. Thermal collapse of the carbon-rich, permafrost-laden coastlines and sea floors may accelerate with Arctic amplification of climate warming, and could further intensify the role of old Ice Complex organic carbon in carbon cycling in the world's largest shelf sea.

METHODS SUMMARY

Surface sediments were collected on several expeditions on the ESAS in 2004, 2005, 2007 and 2008 (Supplementary Fig. 2, Supplementary Tables 1 and 9). The samples were analysed for organic carbon content and $\delta^{13}C$ (UC Davis Stable Isotope Facility, USA) and $\Delta^{14}C$ (US National Ocean Sciences Accelerator Mass Spectrometry (NOSAMS) Facility of the Woods Hole Oceanographic Institution, USA). The relative contributions of three endmember sources—Coastal Ice Complex permafrost (ICD-PF: $\delta^{13}C = -26.3 \pm 0.67‰$; $\Delta^{14}C = -940 \pm 84‰$; Supplementary Table 4); topsoil permafrost (topsoil-PF: $\delta^{13}C = -28.2 \pm 1.96‰$; $\Delta^{14}C = -126 \pm 54‰$; Supplementary Table 3); and marine organic carbon ($\delta^{13}C = -24 \pm 3.0‰$, $\Delta^{14}C = 60 \pm 60‰$; Supplementary Figs 4, 5)—to the surface sediment organic carbon content were quantified using a dual-carbon-isotope mixing model, solved with a Monte Carlo simulation approach (Supplementary Table 3). Radiochronological measurements on sediment cores from the ESAS were performed at Stockholm University and at the Radiation Research Division of the Risø National Laboratory for Sustainable Energy, Denmark (Supplementary Table 10, Supplementary Fig. 3). Total inventories of excess ^{210}Pb were used to calculate the annual sediment organic carbon accumulation on the ESAS (Supplementary Table 2). The average contribution of organic carbon from ICD-PF in the surface sediment was then used to infer the annual sediment organic carbon accumulation from ICD-PF to the ESAS.

Ice Complex samples from the slopes of Muostakh Island were collected in July 2006 (Fig. 3, Supplementary Table 7). Bulk organic carbon and $\delta^{13}C$ analyses were performed at Stockholm University (Department of Geological Sciences) and $\Delta^{14}C$ analyses at NOSAMS. The soil samples were extracted and separated for identification of molecular biomarkers using gas chromatography/mass spectrometry. In addition, soil respiration measurements were collected on Muostakh Island slopes with automatic lid chambers equipped with infrared gas analysers (Fig. 3; Supplementary Table 8). Full details of methods are available in Supplementary Methods.

Received 1 December 2011; accepted 3 July 2012.
Published online 29 August 2012.

1. Friedlingstein, P. *et al.* Climate-carbon cycle feedback analysis: results from the C^4MIP model intercomparison. *J. Clim.* **19,** 3337–3353 (2006).
2. Solomon, S. D, *et al.* (eds) *Climate Change 2007: The Physical Science Basis* (Cambridge Univ. Press, 2007).
3. Gruber, N. *et al.* in *The Global Carbon Cycle: Integrating Humans, Climate and the Natural World*, (eds Field, C. B. & Raupach, M. R.) 45–76 (Island Press, 2004).
4. Zimov, S. A., Schuur, E. A. G. & Chapin, F. S. III. Permafrost and the global carbon budget. *Science* **312,** 1612–1613 (2006).
5. Schirrmeister, L. *et al.* Sedimentary characteristics and origin of the Late Pleistocene Ice Complex on north-east Siberian Arctic coastal lowlands and islands – a review. *Quat. Int.* **241,** 3–25 (2011).
6. Soloviev, V. A., Ginzburg, G. D., Telepnev, E. V. & Mikhaluk, Y. N. *Cryothermia of Gas Hydrates in the Arctic Ocean* (VNIIOkeangeologia, 1987).
7. Shakhova, N. *et al.* Extensive methane venting to the atmosphere from sediments of the East Siberian Arctic Shelf. *Science* **327,** 1246–1250 (2010).
8. Tarnocai, C. *et al.* Soil organic carbon pools in the northern circumpolar permafrost region. *Glob. Biogeochem. Cycles* **23,** GB2023 (2009).
9. Schuur, E. A. G. *et al.* The effect of permafrost thaw on old carbon release and net carbon exchange from tundra. *Nature* **459,** 556–559 (2009).
10. Rivkina, E., Gilichinsky, D., Wagener, S., Tiedje, J. & McGrath, J. Biogeochemical activity of anaerobic microorganisms from buried permafrost sediments. *Geomicrobiol. J.* **15,** 187–193 (1998).
11. Dutta, K., Schuur, E. A. G., Neff, J. C. & Zimov, S. A. Potential carbon release from permafrost soils of Northeastern Siberia. *Glob. Change Biol.* **12,** 2336–2351 (2006).
12. Richter-Menge, J. & Overland, J. E. (eds) *Arctic Report Card 2010*, http://www.arctic.noaa.gov/reportcard (2010).
13. Dmitrenko, I. A. *et al.* Recent changes in shelf hydrography in the Siberian Arctic: potential for subsea permafrost instability. *J. Geophys. Res.* **116,** C10027 (2011).
14. Stein, R. & Macdonald, R. W. *The Organic Carbon Cycle in the Arctic Ocean* (Springer, 2004).
15. Mastepanov, M. *et al.* Large tundra methane burst during onset of freezing. *Nature* **456,** 628–630 (2008).
16. Nicolsky, D. & Shakhova, N. Modeling sub-sea permafrost in the East Siberian Arctic Shelf: the Dmitry Laptev Strait. *Environ. Res. Lett.* **5,** 015006 (2010).
17. Romanovskii, N. N., Hubberten, H.-W., Gavrilov, A. V., Eliseeva, A. A. & Tipenko, G. S. Offshore permafrost and gas hydrate stability zone on the shelf of East Siberian Seas. *Geo-Mar. Lett.* **25,** 167–182 (2005).
18. Grigoriev, M. N. *Cryomorphogenesis and Lithodynamics of the Coastal-shelf Zone of the Seas of Eastern Siberia*. Doctoral thesis, Yakutsk Melnikov Permafrost Inst. (2008).
19. Semiletov, I. P. The failure of coastal frozen rock as an important factor in the biogeochemistry of the Arctic shelf water. *Dokl. Earth Sci.* **369,** 1140–1143 (1999).
20. Rachold, V. *et al.* Coastal erosion vs riverine sediment discharge in the Arctic Shelf seas. *Int. J. Earth Sci.* **89,** 450–460 (2000).
21. Vonk, J. E. *et al.* Molecular and radiocarbon constraints on sources and degradation of terrestrial organic carbon along the Kolyma paleoriver transect, East Siberian Sea. *Biogeosciences* **7,** 3153–3166 (2010).
22. Overduin, P. P. *et al.* The evolution and degradation of coastal and offshore permafrost in the Laptev and East Siberian Seas during the last climatic cycle. *Geol. Soc. Am. Spec. Pap.* **426,** 97–110 (2007).
23. Keil, R. G., Dickens, A. F., Arnarson, T., Nunn, B. L. & Devol, A. H. What is the oxygen exposure time of laterally transported organic matter along the Washington margin? *Mar. Chem.* **92,** 157–165 (2004).
24. Vonk, J. E., van Dongen, B. E. & Gustafsson, Ö. Selective preservation of old organic carbon fluvially released from sub-Arctic soils. *Geophys. Res. Lett.* **37,** L11605 (2010).
25. Wegner, C. *et al.* Suspended particulate matter on the Laptev Sea shelf (Siberian Arctic) during ice-free conditions. *Estuar. Coast. Shelf Sci.* **57,** 55–64 (2003).
26. Dudarev, O. V., Semiletov, I. P., Charkin, A. N. & Botsul, A. I. Deposition settings on the continental shelf of the East Siberian Sea. *Dokl. Earth Sci.* **409,** 1000–1005 (2006).
27. Sánchez-García, L. *et al.* Inventories and behavior of particulate organic carbon in the Laptev and East Siberian seas. *Glob. Biogeochem. Cycles* **25,** GB2007 (2011).
28. Lantuit, H. *et al.* Towards a calculation of organic carbon release from erosion of Arctic coasts using non-fractal coastline datasets. *Mar. Geol.* **257,** 1–10 (2009).
29. Razumov, S. O. Rates of coastal thermoabrasion as a function of climate and morphological characteristics of the coast. *Geomorphology* **3,** 88–94 (2000).
30. Romanovskii, N. N. *Fundamentals of the Cryogenesis of the Lithosphere* (Moscow University Press, Moscow, 1993).

Supplementary Information is linked to the online version of the paper at www.nature.com/nature.

Acknowledgements We thank all ISSS-08 colleagues and crew, in particular M. Kruså, P. Andersson and V. Mordukhovich, who helped with sampling. The ISSS program is supported by the Knut and Alice Wallenberg Foundation, the Far Eastern Branch of the Russian Academy of Sciences, the Swedish Research Council, the US National Oceanic and Atmospheric Administration, the Russian Foundation of Basic Research, the Swedish Polar Research Secretariat and the Nordic Council of Ministers (Arctic Co-Op and TRI-DEFROST programs). Ö.G. and L.S.-G. acknowledge an Academy Research Fellow grant from the Swedish Royal Academy of Sciences and an EU Marie Curie grant, respectively. N.S. and I.P.S. acknowledge grants from the US National Science Foundation and the NOAA OAR Climate Program Office.

Author Contributions All authors except P.R., T.I.E. and A.A. collected samples. Preparations for bulk organic carbon analyses, stable isotope analysis and radiocarbon analyses were made by J.E.V. (sediments) and L.S.-G. (Ice Complex samples). Radiocarbon analyses on sediments were facilitated by T.I.E. L.S.-G. analysed lipid biomarkers in Muostakh Island samples. A.A. was responsible for the Monte Carlo simulations. Radiochronological measurements on sediment cores were made by P.R. and at Stockholm University. J.E.V. performed data analyses and flux calculations. J.E.V., L.S.-G. and Ö.G. wrote the paper, with input from N.S., I.P.S. and all other authors.

Author Information Reprints and permissions information is available at www.nature.com/reprints. The authors declare no competing financial interests. Readers are welcome to comment on the online version of this article at www.nature.com/nature. Correspondence and requests for materials should be addressed to Ö.G. (orjan.gustafsson@itm.su.se).